



# Theoretical study of diaquamalonatozinc(II) single crystal for applications in non-linear optical devices

MITESH CHAKRABORTY<sup>1,\*</sup> and VINEET KUMAR RAI<sup>2</sup>

<sup>1</sup>Department of Physics, St. Xavier's College, Ranchi 834 001, India

<sup>2</sup>Laser and Spectroscopy Laboratory, Department of Applied Physics, Indian Institute of Technology (Indian School of Mines), Dhanbad 826 004, India

\*Corresponding author. E-mail: mitesh.chakraborty@rediffmail.com

MS received 19 March 2017; revised 6 July 2017; accepted 11 July 2017; published online 28 November 2017

**Abstract.** The aim of the present paper is to employ theoretical methods to investigate the zero field splitting (ZFS) parameter and to investigate the position of the dopant in the host. These theoretical calculations have been compared with the empirical results. The superposition model (SPM) with the microscopic spin-Hamiltonian (MSH) theory and the coefficient of fractional parentage have been employed to investigate the dopant manganese(II) ion substitution in the diaquamalonatozinc(II) (DAMZ) single crystal. The magnetic parameters, viz.  $g$ -tensor and  $D$ -tensor, has been determined by using the ORCA program package developed by F Neese *et al.* The unrestricted Kohn–Sham orbitals-based Pederson–Khanna (PK) as the unperturbed wave function is observed to be the most suitable for the computational calculation of spin–orbit tensor ( $D^{SO}$ ) of the axial ZFS parameter  $D$ . The effects of spin–spin dipolar couplings are taken into account. The unrestricted natural orbital (UNO) is used for the calculation of spin–spin dipolar contributions to the ZFS tensor. A comparative study of the quantum mechanical treatment of Pederson–Khanna (PK) with coupled perturbation (CP) is reported in the present study. The unrestricted Kohn–Sham-based natural orbital with Pederson–Khanna-type of perturbation approach validates the experimental results in the evaluation of ZFS parameters. The theoretical results are appropriate with the experimental ones and indicate the interstitial occupancy of  $Mn^{2+}$  ion in the host matrix.

**Keywords.** Superposition principle; zero field splitting; fractional parentage; principal parent; diaquamalonatozinc(II); non-hybrid functional; basis set.

**PACS No.** 31.5.–p

## 1. Introduction

The electron spin resonance spectroscopy is well-established in multidisciplinary fields to study the characterization of electronic structures of open-shell electrons with non-zero spin [1,2]. Studies using electron magnetic resonance (EMR) spectroscopy or electron spin resonance (ESR) spectroscopy provide information about zero field splitting (ZFS) parameters and local site symmetry of transition metal ions doped in diamagnetic host [3,4]. Studies of electronic structure of impurities in solid materials have attracted great deal of attention of researchers for many years owing to their importance in practical applications [5–9]. The EPR studies on diamagnetic hosts offer detailed information about the electric field symmetry produced by the ligands around the paramagnetic ions [10,11]. In general, paramagnetic ions are doped in diamagnetic or paramagnetic host

lattices of known symmetry [12,13]. The exchange and dipolar interaction between a paramagnetic host and a doped paramagnetic ion broaden the resonance lines and structural studies become difficult. The transition metal ions doped in host lattices play a major role in modifying the crystal structure and have been widely applied in wave guides, holography and electro-optical devices [14,15].

The diaquamalonatozinc(II) abbreviated as DAMZ single crystal, first synthesized in 1982 [16], find its application in the enrichment of dentate ceramics. The structural and spectral investigations of transition metal and rare earth ion complexes doped in the host containing malonato ligands continue to be of current interest for their wide applications. Malonato ligand, when coordinated with platinum, is known in the treatment of malignant tumors (United States Patent 4140707). The complex polymer compounds containing malonic acid

as a ligand have been recently studied due to their potential applications in molecular electronics, catalysts, biologically active compounds, magnetic specimen in molecular form, microporosity, electrical conductivity, non-linear optical activity [17,18] etc.

Manganese(II), abbreviated as Mn(II), doped single crystals have been studied by several researchers [19–22]. The main emphasis of the study was to determine the site symmetry, orientations, phase transitions and magnetic properties of the materials. Mn(II) has five 3d electrons and its ground state is  ${}^6S_{5/2}$ . The S-state ions are characterized by long spin-lattice relaxation times, as the resultant angular momentum is zero. Hence only the electron spin is responsible for the paramagnetic behaviour. The ZFS tensor, its magnitude and orientation being very sensitive to the strength and geometry of the crystal field make these d5 ions ideal to study the site symmetry and phase transitions [23]. Studies of the relaxation behaviour in complexes due to ZFS have attracted considerable interest due to their potential applications in high density information storage, quantum computing and magnetic refrigeration [24–28].

The ZFS may arise due to two types of mechanisms: (1) due to dipole–dipole interaction between the magnetic moments of the unpaired electrons and (2) due to spin–orbit coupling (SOC). In most of the cases, the SOC mechanism was found to be responsible for ZFS in transition metal ions [29]. In the present study, the effect of spin–spin coupling is taken into account. Various techniques such as frequency domain magnetic resonance spectroscopy [30], measurements of the temperature dependence of magnetic susceptibility [31], magnetic circular dichroism [32] and measurements of NMR relaxation rates for nuclear spins associated to a ligand bound to the paramagnetic centre [33] etc. are there to determine the ZFS parameters. The superposition principle using microscopic spin-Hamiltonian (MSH) theory is a simple self-contained quantum mechanical perturbation method based on phenomenological postulates [34,35] to study the axial and rhombic ZFS parameters of the doped paramagnetic ions in host lattices. The superposition model (SPM) developed by Newman and Bradbury was used to separate the geometrical and physical information in the crystal field parameters [36,37]. The SPM has now become an area of active interest for researchers to determine the phenomenological crystal field parameters and dopant position in host compound using MSH [38–40]. Further computer programs based on SPM incorporating Monte–Carlo method has been developed for interpreting EMR spectra [41,42]. The development of theoretical tools to evaluate the ZFS parameters by using quantum chemistry computational models has been studied by Neese *et al* [43–47]. Investigations

by quantum theoretical methods have been reported by some other researchers [48–52].

The present paper deals with the evaluation of ZFS parameter using the theoretical computational program package ORCA developed by Neese *et al*. This computational tool has been previously used to study the ZFS parameters of doped transition metal ions in different hosts [53–55]. This computer program has been used for density functional theory (DFT) with different modules. The  $g$ -tensor, which gives information about the isotropic or anisotropic properties of the crystal, has been computed with ORCA computational program package. The methods of superposition principle and coefficient of fractional parentage have also been used to evaluate the ZFS  $D$  tensor. Previously, the authors have reported the theoretical study on the zero field splitting and dopant position of  $Mn^{2+}$  in potassium trihydrogen selenite single crystal [56].

## 2. Crystal structure

The unit cell of DAMZ is monoclinic with  $a = 1.258$ ,  $b = 0.741$ ,  $c = 0.723$  nm and contains four molecules. From experimental studies it is observed that zinc atom is surrounded by a distorted octahedron of six water molecules, such that the two water molecules are at a distance of 0.206 and 0.215 nm and four oxygen atoms of the two malonato groups are at 0.213 and 0.202 nm [16,57] (figures 1 and 2).

## 3. Theoretical interpretation

In systems with more than one unpaired electrons, the spin degeneracy is removed even in the absence of external magnetic field due to SOC known as the zero field

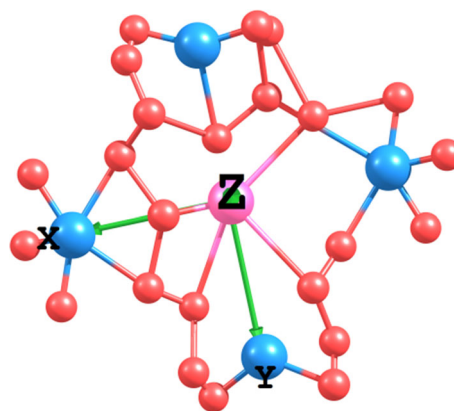


**Figure 1.** The optimized geometrical configuration of the host lattice. The Cartesian coordinates  $X$ ,  $Y$  and  $Z$  are shown. This figure is similar to that given in [16,57]. The red and blue circles indicate the oxygen and zinc(II) atoms respectively. The interstitial position of the manganese impurity is shown as the pink circle.

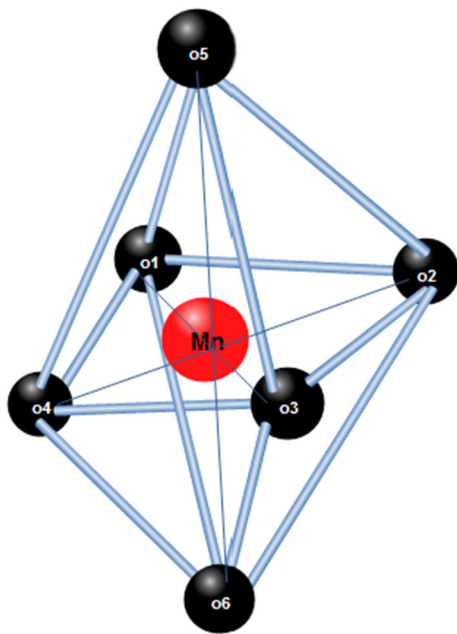


**Figure 2.** Manganese(II) distorted octahedron is expected to occupy any interstitial site. The  $z$ -axis is oriented transverse to the four tetragonal positions of oxygen atoms.

interaction. This is also a dipolar type of interaction that can be expressed as [58]

$$H_{ZFS} = D \left[ S_Z^2 - \frac{1}{3} S(S+1) \right] + E (S_X^2 - S_Y^2), \quad (1)$$

where  $D$  represents the axial zero field splitting parameter and  $E$  is an asymmetry parameter which measures the deviation from axial symmetry.  $E$  is also known as rhombic zero field splitting parameter. In the crystallographic axes frame, the ZFS parameters  $D$  and  $E$  are expressed as

$$D = D_{ZZ} - \frac{1}{2} (D_{XX} + D_{YY}) \quad (2)$$

$$E = \frac{1}{2} (D_{XX} - D_{YY}). \quad (3)$$

This means that the local lattice distortion in the position of the dopant Mn(II) can occur when axial and rhombic ZFSs are present in the host.

From literature survey, it has been observed that the SOC is the most important mechanism for ZFS in the  $Mn^{2+}$ -doped single crystals [59–61]. In the present study, the orbit–orbit interaction is neglected [60]. The ZFS parameters have been evaluated earlier by using the SPM and MSH by considering the local site symmetry to be distorted octahedron [62,63]. From the EPR experimental study of DAMZ single crystal with positive sign of axial ZFS  $D$  and rhombic ZFS  $E$ , the dopant Mn(II) is expected to exhibit compressed octahedron

**Table 1.** Mn(II) interstitial occupancy in the host compound (DAMZ).

Mn–O bond length (Å)	$\Theta$ (°)	$\Phi$ (°)
2.74(O <sub>3</sub> )	90.01	90
2.56(O <sub>2</sub> )	91.07	180
2.54(O <sub>4</sub> )	91.07	0
2.76(O <sub>1</sub> )	87.85	270
3.23(O <sub>5</sub> )	0	0
3.22(O <sub>6</sub> )	180	0

(i.e. orthorhombically distorted) [57]. Since the ionic radii of Mn(II) and Zn(II) are different, a reasonable change is made in the bond length and bond angles of Mn–O.

### 3.1 MSH Theory

The system is considered to be perturbed with tetragonal symmetry, and the axial ZFS parameter  $D$  and rhombic ZFS parameter  $E$  can be expressed as [60],

$$\begin{aligned} D^{(4)}(\text{SO}) &= (3\xi^2/70P^2D)(-B_{20}^2 - 21\xi B_{20} + 2B_{22}^2) \\ &\quad + (\xi^2/63P^2G)(-5B_{40}^2 - 4B_{42}^2 - 14B_{44}^2) \\ E^{(4)}(\text{SO}) &= (\sqrt{6}\xi^2/70P^2D)(2B_{20} - 21\xi)B_{22} \\ &\quad + (\xi^2/63P^2G)(3\sqrt{10}B_{40} + 2\sqrt{7}B_{44})B_{42} \end{aligned} \quad (4)$$

where

$$P = 7W + 7C, G = 10W + 5C, D = 17W + 5C.$$

The parameter  $W$  measures the interelectronic repulsion among the electrons in the d-orbitals. The values of  $W$  and  $C$  are the measures of the spatial arrangement of the orbitals between the ligand and the metal ion. The effect of spin–orbit interaction to the Hamiltonian is considered in the above expression. In consideration with the nephelauxetic effect in terms of average covalency factor  $N$ , the Racah parameters  $W$  and  $C$  are expressed as  $W = N^4W_0$  and  $C = N^4C_0$ , where  $W_0$  and  $C_0$  signify Racah parameters in the free state. The SOC would be reduced in a crystal by a factor  $\xi_d = N^2\xi_d^0$ .

The proposed polar coordinate ( $\Theta$ ) and bond lengths (Å) for  $Mn^{2+}$  interstitial occupancy in DAMZ evaluated from X-ray diffraction (XRD) study [16] are given in table 1. The bond lengths and angles have been varied because the ionic radii of  $Mn^{2+}$  and  $Zn^{2+}$  are different.

### 3.2 Results and discussion

All calculations have been done in the symmetry adapted axis system. The phenomenological crystal field param-

eters evaluated are as follows:  $B_{20} = 13183 \text{ cm}^{-1}$ ,  $B_{22} = 22 \text{ cm}^{-1}$ ,  $B_{40} = 1345.8 \text{ cm}^{-1}$ ,  $B_{42} = -13.49 \text{ cm}^{-1}$ . The calculated values of axial ( $D$ ) and rhombic ( $E$ ) zero field splitting parameters are  $546 \times 10^{-4} \text{ cm}^{-1}$  and  $124 \times 10^{-4} \text{ cm}^{-1}$  respectively.

## 4. DFT computational studies

### 4.1 Computational details

All calculations of the ZFS parameters  $D$  and  $E$  of the dopant in the base compound DAMZ were performed using the ORCA program package [64–66]. The non-hybrid functional BP and hybrid functional B3LYP are reported in the present investigation. The basis set def2-TZVP is used in conjunction with auxiliary basis set def2-TZVP/J. In the present calculation, the SOC operator has been represented by the spin-orbit mean-field (SOMF) method [67–69]. The COSMO model is used for dielectric modelling of the environment. Water solvent is used for environmental effects. Zeroth-order regular approximation (ZORA) is taken into account to

consider relativistic effects. The SOC calculation is performed by both coupled-perturbed (CP) and Pederson–Khanna (PK) methods which utilize the single determinant wave function consisting of unrestricted natural orbitals (UNO) for spin–spin dipolar coupling. Both these methods are incorporated in ORCA software package.

### 4.2 Results and discussion

The principal values of the D-Tensor evaluated from non-hybrid functional BP and hybrid functional B3LYP are reported in table 2. The computation based on non-hybrid functional is in agreement with the experimental results. From table 2, it is clear that the evaluation based on the unrestricted Kohn–Sham orbitals with Pederson–Khanna (PK) as the unperturbed wave function is observed to be the most suitable in the computational calculation of spin–orbit tensor ( $D^{\text{SO}}$ ) of the axial ZFS parameter  $D$  for non-hybrid functional BP. The computation results also reveal that spin–spin coupling contribution to the  $D$  tensor ( $D^{\text{SS}}$ ) is non-zero and should be taken into consideration [70–72]. In view of the results

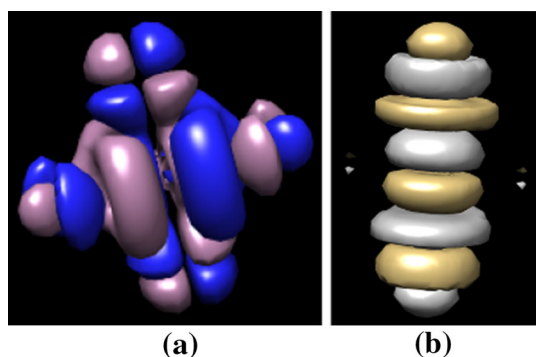


**Figure 3.** The orbital plots of spin–spin dipolar coupling ( $D^{\text{SS}}$ ) for Mn(II) ion with d5 configuration doped in DAMZ single crystal visualized with UCSF Chimera molecular visualization software. (a)  $\alpha$ -spin (up-spin) and (b)  $\beta$ -spin (down-spin).

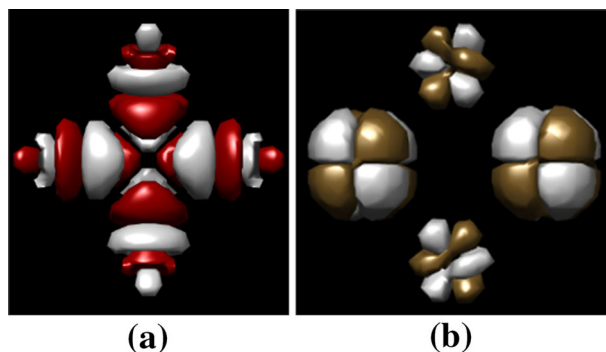


**Figure 4.** The orbital plot of ZFS parameter  $D^{\text{Total}}$  constituting the spin–orbit and spin–spin coupling for Mn(II) ion with d5 configuration doped in DAMZ single crystal visualized with UCSF Chimera molecular visualization software. (a)  $\alpha$ -spin (up-spin) and (b)  $\beta$ -spin (down-spin).

**Table 2.** Calculated principal values of  $D$  ( $\text{cm}^{-1}$ ) for the doped DAMZ single crystal obtained using hybrid and non-hybrid functionals.

$\text{cm}^{-1}$	Non-hybrid functional		Hybrid functional		Experimental [55]
	BP		B3LYP		
	CP+UNO	PK+UNO	CP+UNO	PK+UNO	
$D^{\text{SO}} \times 10^{-4}$	833.58	626.66	1447.56	1329.33	
$D^{\text{SS}} \times 10^{-4}$	-389.24	-349.24	-786.33	-689.34	
$D^{\text{Total}} \times 10^{-4}$	-694.88	-584.33	-1339.56	-1256.77	571
$E/D$	0.0589	0.177	0.023	0.149	0.210

from table 2 for the dopant Mn(II) ion in the present host DAMZ we rely on non-hybrid functional BP. For all the above calculations from DFT, the rhombic ZFS parameter  $E$  is found to be significant in comparison to  $D$  but limited to the convention ( $E/D \leq 1/3$ ). This shows the high axial symmetry of the dopant ion about the nearest-neighbour oxygen atoms. The computed values of  $g_{xx}$  (2.0018),  $g_{yy}$  (2.0014) and  $g_{zz}$  (2.0039) are different confirming the existence of axial and rhombic distortions in the local site symmetry of the Mn(II) ion. The SOC is mainly due to four factors: (i) excitation of a singly occupied molecular orbital (SOMO) to a virtual molecular orbital (VMO) which leads to the same spin-up state ( $\alpha$ ) of the electron ( $\alpha \rightarrow \alpha$ ), (ii) excitation from a doubly occupied molecular orbital (DOMO) to a singly occupied molecular orbital (SOMO) with the same spin-down state ( $\beta$ ) of the electron ( $\beta \rightarrow \beta$ ), (iii)

within the same SOMO the spin-flip excitation is represented by  $\alpha \rightarrow \beta$ , (iv) the spin-flip transition from a VMO to SOMO is given by  $\beta \rightarrow \alpha$  [71]. The magnitude of  $\alpha \rightarrow \beta$  transition is found to be maximum for axial ZFS parameter  $D$  and rhombic ZFS parameter  $E$ . The magnitude of  $\beta \rightarrow \alpha$  transition and  $\alpha \rightarrow \alpha$  transition is minimum for axial and rhombic ZFS parameter  $D$  and  $E$  respectively. The results seems to validate the argument that maximum valence  $d \rightarrow d$  transitions are attributed to  $\alpha \rightarrow \beta$  excitation because the dopant Mn(II) ion has electronic configuration  $d^5$  and therefore all valence 3d orbitals are occupied by  $\alpha$ -spin in the high-spin spin-sextet state. The orbital plots of high spin d states for Mn(II) dopant in the host DAMZ single crystal with spin-spin dipolar coupling and the total perturbation due to spin-orbit and spin-spin coupling are reported in figure 3 and figure 4 respectively [72]. The molecular

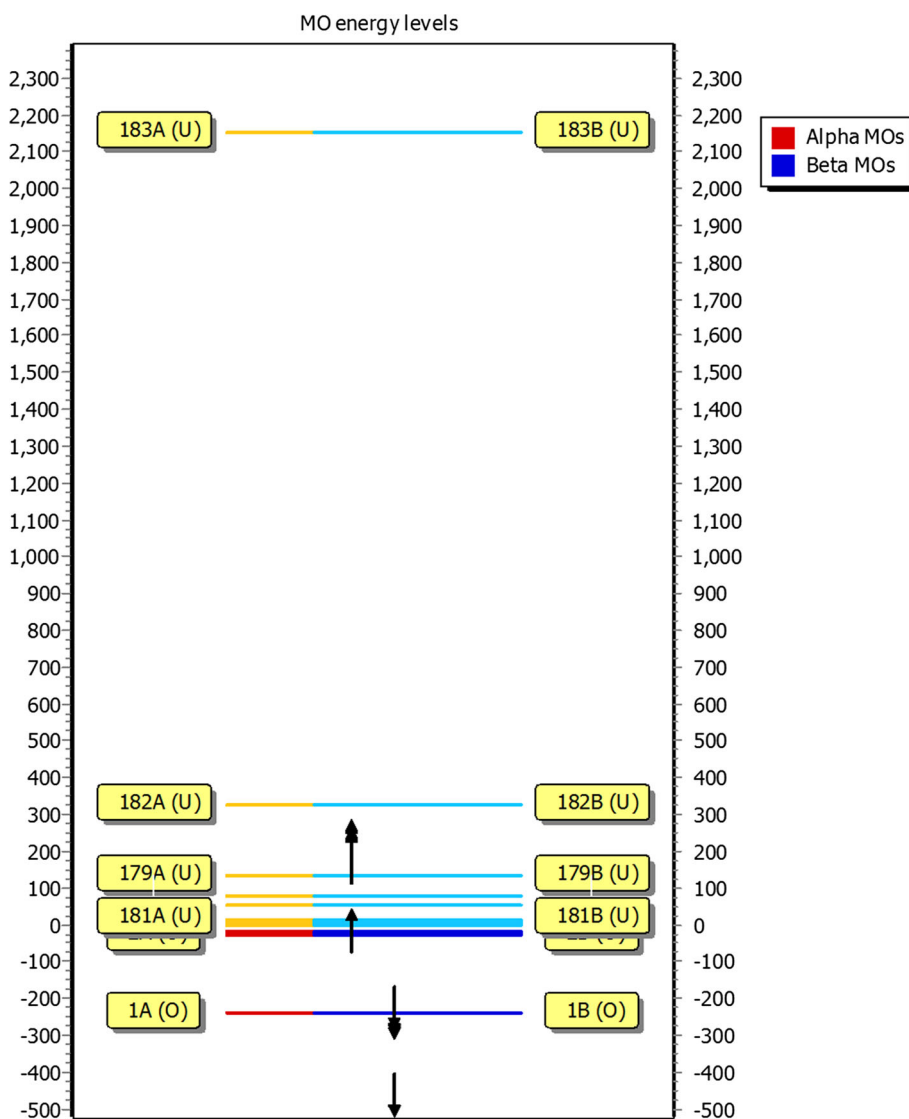


**Figure 5.** The molecular orbital energy level diagram for the dopant ion in the host DAMZ for the non-hybrid functional BP.

orbital (MO) energy level diagram for the dopant Mn(II) ion in the host DAMZ for the BP non-hybrid functional is presented in figure 5. In the given block diagrams the up arrows represent the upward electron spin and the down arrows signify the downward electron spin. The O mark shows the occupied orbital and U mark shows the unoccupied orbital. The symbols A and B are for alpha and beta energy respectively.

## 5. Coefficient of fractional parentage

The coefficient of fractional parentage is a quantum mechanical tool to obtain antisymmetric many-body states for similar types of particles. The ZFS parameters are evaluated using coefficient of fractional parentage [73]. The Hamiltonian for the d5 ion configuration in octahedral symmetry is expressed as

$$H = H_0 + H_{CF} + H_{so}, \quad (5)$$

where  $H_0$  denotes the electrostatic interaction,  $H_{SO}$  is the spin-orbit coupling interaction and  $H_{CF}$  is the crystal field potential. The crystal field for tetragonal symmetry in terms of Wybourne notation is as follows [74]:

$$H_{CF} = B_{20}C_0^{(2)} + B_{40}C_0^{(4)} + B_{44} \left( C_4^{(4)} + C_{-4}^{(4)} \right). \quad (6)$$

Since the interaction between the ligand field and transition metal ions is weak in the crystal, the basis of states in the LS coupling scheme can be stated as [75]

$$|\psi\rangle = |d^n \alpha S M_S L M_L\rangle,$$

where  $\alpha$  is an extra quantum number and  $d = l = 2$  in accordance with the spectroscopic notation in atomic theory. Hence the matrix elements due to crystal field interaction operations are evaluated as follows:

$$\langle \psi | H_{CF} | \psi' \rangle = \sum B_{kq} \langle \psi | C_q^{(k)} | \psi' \rangle \quad (7)$$

and

$$\langle \psi | C_q^{(k)} | \psi' \rangle = (-1)^{L-M_L} \begin{pmatrix} L & k & L' \\ -M & q & M' \end{pmatrix} \times \langle \beta || C^k || \beta' \rangle \delta_{S'S'} \delta_{M_S M_{S'}}, \quad (8)$$

where

$$\beta = d^n \alpha L S$$

and

$$\langle \beta || C^k || \beta' \rangle = \langle d || C^k || d \rangle \langle \beta || U^k || \beta' \rangle \quad (9)$$

where

$$\langle d || C^k || d \rangle = (-1)^d (2d+1) \begin{pmatrix} d & k & d \\ 0 & 0 & 0 \end{pmatrix}, \quad d = 2. \quad (10)$$

The reduced matrix elements for the unit tensor operator  $\|U^K\|$  are calculated in Appendix II.

$$\begin{aligned} \langle \psi | H_{so} | \psi' \rangle &= \xi \times (-1)^{S+L-M_S-M_L} \\ &\times \langle d^n \alpha L S || V^{11} || d^n \alpha' L' S' \rangle \\ &\times [(2l+1)(l+1)l]^{1/2} \sum_q (-1)^q \\ &\times \begin{pmatrix} S & 1 & S' \\ -M_S & q & M_{S'} \end{pmatrix} \\ &\times \begin{pmatrix} L & 1 & L' \\ -M & -q & M' \end{pmatrix} \end{aligned} \quad (11)$$

where  $2 \times 3$  denotes the 3-j symbol and the reduced matrix elements  $\|V^{11}\|$  are calculated explicitly according to the formula given in Appendix II [76–79].

## 6. Conclusion

The theoretical evaluations of axial ZFS parameter agree reasonably well with the empirical results. Since  $g_{xx} \neq g_{yy} \neq g_{zz}$ , the system exhibits axial symmetry with rhombic distortion. The computation of axial and rhombic ZFS parameters  $D$  and  $E$  is reported for the non-hybrid functional BP and the hybrid functional B3LYP. The non-hybrid functional BP with the basis set def2-TZVP used in conjunction with auxiliary basis set def2-TZVP/J for Mn(II)-doped complexes provides reasonable estimation of ZFS parameters. The phenomenological crystal field parameters have been determined using superposition principle. The coefficient of fractional parentage with the principal parent  ${}^6S$  has been employed to verify the dopant's position in the base compound. Based on the theoretical observations it is reported that Mn(II) occupy interstitial sites.

## Acknowledgements

The authors express their sincere thanks to S Deepa and B Natarajan for considering their request to study the empirical work on DAMZ crystal by theoretical methods published in the *IOSR Journal of Applied Chemistry* 7 (2014) 57, *J. Mol. Struc.* **839** (2007) 2–9. The authors are grateful to the Science and Engineering Research Board (SERB), DST, New Delhi, India for providing financial assistance in the form of a project (EMR/2014/001273).

### Appendix I

$$\begin{aligned}
 B_{20} &= \overline{A_2}(R_0) \left[ \begin{aligned} &(R_0/R_1)^{t_2}(3 \cos^2 \theta_1 - 1) + (R_0/R'_1)^{t_2}(3 \cos^2 \theta'_1 - 1) \\ &+ (R_0/R_2)^{t_2}(3 \cos^2 \theta_2 - 1) + (R_0/R'_2)^{t_2}(3 \cos^2 \theta'_2 - 1) \end{aligned} \right], \\
 2B_{22} &= \sqrt{6A_2}(R_0) \left[ \begin{aligned} &(R_0/R_1)^{t_2} \sin^2 \theta_1 \cos(2\phi_1) + (R_0/R'_1)^{t_2} \sin^2 \theta'_1 \cos(2\phi'_1) \\ &+ (R_0/R_2)^{t_2} \sin^2 \theta_2 \cos(2\phi_2) + (R_0/R'_2)^{t_2} \sin^2 \theta'_2 \cos(2\phi'_2) \end{aligned} \right], \\
 B_{40} &= \overline{A_4}(R_0) \left[ \begin{aligned} &(R_0/R_1)^{t_4}(35 \cos^4 \theta_1 - 30 \cos^2 \theta_1 + 3) \\ &+ (R_0/R'_1)^{t_4}(35 \cos^4 \theta'_1 - 30 \cos^2 \theta'_1 + 3) \\ &+ (R_0/R_2)^{t_4}(35 \cos^4 \theta_2 - 30 \cos^2 \theta_2 + 3) \\ &+ (R_0/R'_2)^{t_4}(35 \cos^4 \theta'_2 - 30 \cos^2 \theta'_2 + 3) \end{aligned} \right], \\
 B_{42} &= \sqrt{10A_4}(R_0) \left[ \begin{aligned} &(R_0/R_1)^{t_4} \sin^2 \theta_1 (7 \cos^2 \theta_1 - 1) \cos(2\phi_1) \\ &+ (R_0/R'_1)^{t_4} \sin^2 \theta'_1 (7 \cos^2 \theta'_1 - 1) \cos(2\phi'_1) \\ &+ (R_0/R_2)^{t_4} \sin^2 \theta_2 (7 \cos^2 \theta_2 - 1) \cos(2\phi_2) \\ &+ (R_0/R'_2)^{t_4} \sin^2 \theta'_2 (7 \cos^2 \theta'_2 - 1) \cos(2\phi'_2) \end{aligned} \right], \\
 2B_{44} &= \sqrt{70A_4}(R_0) \left[ \begin{aligned} &(R_0/R_1)^{t_4} \sin^4 \theta_1 \cos(4\phi_1) \\ &+ (R_0/R'_1)^{t_4} \sin^4 \theta'_1 \cos(4\phi'_1) \\ &(R_0/R_2)^{t_4} \sin^4 \theta_2 \cos(4\phi_2) \\ &+ (R_0/R'_2)^{t_4} \sin^4 \theta'_2 \cos(4\phi'_2) \end{aligned} \right].
 \end{aligned}$$

### Appendix II

The reduced matrix elements for the orbital tensor unit operators and the double tensor operators are evaluated using coefficient of fractional parentage  $\langle l^n, \alpha SL \{ |l^{n-1} \alpha' S' L' \rangle$

$$\begin{aligned}
 &\langle l^n \alpha LS \| U^k \| l^n \alpha' L' S' \rangle \\
 &= n [(2L + 1)(2L'' + 1)]^{1/2} \cdot \delta_{SS'} \\
 &\quad \times \sum_{\alpha'' S'' L''} (-)^{L+L''+l+k} \begin{pmatrix} l & l & k \\ L' & L & L'' \end{pmatrix} \\
 &\quad \times \langle l^n, \alpha SL \{ |l^{n-1} \alpha'' S'' L'' \rangle \\
 &\quad \times \langle l^n, \alpha' S' L' \{ |l^{n-1} \alpha'' S'' L'' \rangle \\
 &\langle l^n \alpha LS \| V^{lk} \| l^n \alpha' L' S' \rangle \\
 &= n [(2L + 1)(2S + 1)]^{1/2} [(2L' + 1)(2S' + 1)]^{1/2} \\
 &\quad \times \sqrt{3/2} \sum_{\alpha'' L'' S''} (-)^{L+L''+l+k+S+S'+3/2} \\
 &\quad \times \begin{pmatrix} S & S' & 1 \\ 1/2 & 1/2 & S'' \end{pmatrix}, \begin{pmatrix} l & l & k \\ L' & L & L'' \end{pmatrix} \\
 &\quad \times \langle l^n, \alpha SL \{ |l^{n-1} \alpha'' S'' L'' \rangle \\
 &\quad \times \langle l^n, \alpha' S' L' \{ |l^{n-1} \alpha'' S'' L'' \rangle.
 \end{aligned}$$

### References

- [1] A Abragam and B Bleaney, *Electron paramagnetic resonance of transition ions* (Clarendon Press, Oxford, 1970)
- [2] W R Hagen, *Biomolecular EPR spectroscopy* (CRC Press, Taylor & Francis Group, Boca Raton, FL, 2009)
- [3] J A Weil and J R Bolton, *Electron paramagnetic resonance: Elementary theory and practical applications* (Wiley, New York, 2007)
- [4] F E Mabbs and D Collison, *Electron paramagnetic resonance of d transition metal compounds* (Elsevier, Amsterdam, 1992)
- [5] X Gratsens, S Isber and S Charar, *Phys. Rev. B* **76**, 035203 (2007)
- [6] M Moreno, J M Garcia-Lastra, M T Barriuso and J A Aramburu, *Theor. Chem. Acc.* **118**, 665 (2007)
- [7] M Moreno, *J. Phys. Chem. Solids* **51**, 835 (1990)
- [8] J A Aramburu, J I Paredes, M T Barriuso and M Moreno, *Phys. Rev. B* **61**, 6525 (2000)
- [9] F A Mikailov, B Z Rameev, S Kazan, F Yildiz and B Aktaş, *Solid State Commun.* **135**, 114 (2005)
- [10] H Kalkan and F Koksall, *Solid State Commun.* **105**, 307 (1998)
- [11] R S Bansal, V P Seth, P Chand and S K Gupta, *J. Phys. Chem. Solids* **52**, 389 (1991)
- [12] S K Misra, S I Andronenko, G Rinaldi, P Chand, K A Earle and J H Freed, *J. Magn. Reson.* **160**, 131 (2003)
- [13] C L Raju, N O Gopal, K V Narasimhulu, J L Rao and B C V Reddy, *Spectrochim. Acta A* **61**, 2181 (2005)

- [14] L S R Prasad and S Subramanian, *J. Chem. Phys.* **83**, 1485 (1985)
- [15] W C Zheng, *Phys. Status Solidi B* **205**, 627 (1998)
- [16] Noel J Ray and Brian J Hathaway, *Acta Cryst. B* **38**, 770 (1982)
- [17] C Ruiz-Perez, Y Rodriguez-Martin, M Hernandez-Molina, F S Delgado, J Pasan, J Sanchiz, F Lloret and M Julve, *Polyhedron* **22**, 2111 (2003)
- [18] J Pasan, F S Delgado, Y Rodriguez-Martin, M Hernandez-Molina, C Ruiz-Perez, J Sanchiz, F Lloret and M Julve, *Polyhedron* **22**, 2143 (2003)
- [19] D P Pandiyan, C Muthukrishnan and R Murugesan, *Spectrochim. Acta (Part A)* **58**, 509 (2002)
- [20] T K Gundu and P Manoharan, *Chem. Phys. Lett.* **264**, 338 (1997)
- [21] B Wagner, S A Warda, M A Hitchman and D Rienen, *Inorg. Chem.* **35**, 3967 (1996)
- [22] J Lech, A Slezak and R Harbanski, *J. Phys. Chem. Solids* **52**, 685 (1991)
- [23] P S Rao and S Subramanian, *Mol. Phys.* **54**, 429 (1985)
- [24] M H Jo, J E Baheti, M M Deshmukh, J J Sokol, E M Rumberger, D Hendrickson, J R Long, H Park and D C Ralph, *Nano Lett.* **6**, 2014 (2006)
- [25] L Bogani and W Wernsdorfer, *Nat. Mater.* **7**, 179 (2008)
- [26] S Loth, K V Bergmann, M Ternes, A F Otte, C P Lutz and A J Heinrich, *Nat. Phys.* **6**, 340 (2010)
- [27] P C E Stamp and A Gaita, *J. Mater. Chem.* **19**, 1718 (2009)
- [28] M N Leuenberger and D Loss, *Nature* **410**, 789 (2001)
- [29] J S Griffith, *The theory of transition-metal ions* (Cambridge University Press, Cambridge, 1961)
- [30] N Kirchner, J van Slageren and M Dressel, *Inorg. Chim. Acta* **360**, 3813 (2007)
- [31] J N Rebilly, G Charron, E Riviere, R Guillot, A L Barra, M D Serrano, J van Slageren and T Mallah, *J. Eur. Chem.* **14**, 1169 (2008)
- [32] J Krzystek, S A Zvyagin, A Ozarowski, A T Fiedler, T C Brunold and J Telser, *J. Am. Chem. Soc.* **126**, 2148 (2004)
- [33] D Kruk, J Kowalewski, D S Tipikin, J H Freed, M Mosciacki, A Mielczarek and M Port, *J. Chem. Phys.* **134**, 024508 (2011)
- [34] W L Yu and M G Zhao, *Phys. Status Solidi B* **140**, 203 (1987)
- [35] W L Yu and M G Zhao, *Phys. Rev. B* **37**, 9254 (1988)
- [36] D J Newman and B T Ng, *Rep. Prog. Phys.* **52**, 699 (1989)
- [37] D J Newman and B T Ng, *Crystal field handbook* (Cambridge University Press, Cambridge, 2000)
- [38] R Kripal and D Yadav, *Solid State Commun.* **150**, 1621 (2010)
- [39] M G Mishra and R Kripal, *Mol. Phys.* **110**, 3001 (2012)
- [40] T H Yeom, S H Choh, M L Du and M S Jang, *Phys. Rev. B* **53**, 6 (1996)
- [41] I Stefaniuki and C Rudowicz, *Curr. Topics Biophys.* **33**, 217 (2010)
- [42] I Stefaniuki and C Rudowicz, *Nukleonika* **58**, 397 (2013)
- [43] F Neese, *Coord. Chem. Rev.* **253**, 526 (2009)
- [44] F Neese and E Solomon, *Inorg. Chem.* **37**, 6568 (1998)
- [45] D Ganyushin and F Neese, *J. Chem. Phys.* **125**, 024103 (2006)
- [46] D G Liakos, D Ganyushin and F Neese, *Inorg. Chem.* **48**, 10572 (2009)
- [47] M Sundarajan, D Ganyushin, S F Ye and F Neese, *Dalton Trans.* **1**, 6021 (2009)
- [48] F Aquino and J H Rodriguez, *J. Chem. Phys.* **123**, 204902 (2005)
- [49] F Aquino and J H Rodriguez, *J. Phys. Chem. A* **113**, 9150 (2009)
- [50] T Yoshizawa and T Nakazima, *Chem. Phys. Lett.* **515**, 296 (2011)
- [51] M P S Yadav and A Kumar, *Pramana – J. Phys.* **89**, 18 (2017)
- [52] A Kumar and M P S Yadav, *Pramana – J. Phys.* **89**, 7 (2017)
- [53] S Dutta and R C Deka, *Comput. Theor. Chem.* **1072**, 1 (2015)
- [54] J Martes, H Liimatainen, K Laasonen and J Vaara, *J. Chem. Theory Comput.* **7**, 3248 (2011)
- [55] R Maurice, L Vendier and J P Costes, *Inorg. Chem.* **50**, 11075 (2011)
- [56] M Chakraborty, V K Rai and V Mishra, *Optik* **127**, 4333 (2016)
- [57] S Deepa and B Natarajan, *IOSR J. Appl. Chem.* **7**, 57 (2014)
- [58] W L Yu and M G Zhao, *Phys. Rev. B* **37**, 9254 (1988)
- [59] W C Zheng, *Phys. Rev. B* **42**, 826 (1990)
- [60] W L Yu, M G Zhao and Z Q Lin, *J. Phys. C* **18**, 1857 (1985)
- [61] W L Yu, *Phys. Rev. B* **41**, 9415 (1990)
- [62] Y W Lun and C Rudowicz, *Phys. Rev. B* **45**, 17 (1992)
- [63] R Kripal and M Singh, *Spectrochim. Acta Part A: Mol. Biomol. Spec.* **135**, 865 (2015)
- [64] F Neese, ORCA – An Ab Initio, Density Functional and Semiempirical Program Package, version 3.0.1, Max-Planck-Institute Max-Planck-Institute for Chemische Energiekonversion, Germany
- [65] F Neese, *Wiley Interdisciplinary Reviews – Computational Molecular Science* **2**, 73 (2012)
- [66] M Atanasov, D Aravena, E Suturina, E Bill, D Maganas and F Neese, *Coord. Chem. Rev.* **289**, 177 (2015)
- [67] B A Hess, C M Marian, U Wahlgren and O Gropen, *Chem. Phys. Lett.* **251**, 365 (1996)
- [68] A D Becke, *Phys. Rev. A* **38**, 3098.F (1988)
- [69] S Zein, C Duboc, W Lubitz and F Neese, *Inorg. Chem.* **47**, 134 (2008)
- [70] C Duboc, T Phoeung, S Zein, J Peacut, M Collomb and F Neese, *Inorg. Chem.* **46**, 4905 (2007)
- [71] K Sugisaki, K Toyota, K Sato, D Shiomi and T Takui, *J. Phys. Chem. A* **120**, 9857 (2016)

- [72] E F Pettersen, T D Goddard, C C Huang, G S Couch, D M Greenblatt, E C Meng and T E Ferrin, *J. Comput. Chem.* **25**, 1605 (2004)
- [73] E U Condon and H Udabasi, *Atomic Structure*, CUP Archive, 1980
- [74] W Qun, *Solid State Commun.* **138**, 427 (2006)
- [75] Z Y Yang, *Appl. Magn. Reson.* **18**, 455 (2000)
- [76] C W Neilson and G F Koster, *Spectroscopic coefficients for the  $p^n$ ,  $d^n$  and  $f^n$  configurations* (Cambridge University Press, Cambridge, 1963)
- [77] C Rudowicz and Y Wan-lun, *J. Phys. Condens. Matter* **3**, 8225 (1991)
- [78] Y Y Yeung and C Rudowicz, *Comp. Chem.* **16**, 207 (1992)
- [79] Y M Chang, C Rudowicz and Y Y Yeung, *Comput. Phys.* **8**, 583 (1994)